Electrochimica Acta 55 (2010) 1373–1379

Contents lists available at ScienceDirect

Electrochimica Acta

journal homepage: www.elsevier.com/locate/electacta

Titanium dioxide/amine hybrid nanotubes. Optical properties and behavior as lithium–ion electrode

Juan Vasquez[a,b], Zoraya López[a], Alejandro Zuñiga[a], Ana Nacher[c], Mónica Lira-Cantú[c], Pedro Gómez-Romero[c], María Angélica Santa Ana[a], Eglantina Benavente[b], Guillermo González[a,*]

[a] Universidad de Chile, P.O. Box 653, Santiago, Chile
[b] Universidad Tecnológica Metropolitana, P.O. Box 9845, Santiago, Chile
[c] Centre d'Investigacions en Nanociència i Nanotecnologia, CIN2, Campus UAB, 08193 Bellaterra, Barcelona, Spain

ARTICLE INFO

Article history:
Received 20 October 2008
Received in revised form 1 May 2009
Accepted 6 May 2009
Available online 13 May 2009

Keywords:
TiO_2 nanostructures
H_2Ti3O_7 nanotubes
Hybrid TiO_2 nanocomposites
Lithium intercalation
Optical properties

ABSTRACT

Titanium dioxide based tubular nanocomposites containing long-chain amines were prepared by hydrothermal reaction of anatase with neutral surfactants, dodecylamine and octadecylamine, under strong alkaline conditions. Morphologically pure phases are obtained after reaction times of about 50 h at 130 °C. Dodecylamine derivates are structural and thermally more fragile than those with octadecylamine. Under more drastic reaction conditions, 72 h at 150 °C, amine is segregated leading to almost pure inorganic nanotubes or fibers for octadecyl and dodecyl derivatives respectively. The products characterized by electron microscopy, X-ray diffraction, FT-IR and elemental analysis are constituted by the hydrogen titanat $H_2Ti_3O_7$. Diffuse reflectance spectra reveal the products present typical size-dependent optical properties. The photoluminescence spectra are qualitatively similar to that of anatase dominated by the presence of traps located in the band gap. The electrochemical lithium intercalation and lithium diffusion coefficients of the products were studied by intermittent galvanostatic method and galvanostatic pulse relaxation technique respectively. Products were tested in a lithium cell using the nanocomposites as the active material of the positive electrode. The hybrid dodecylamine derivative shows a first cycle irreversible capacity of 219 mAh/g, and a capacity of 113 mAh/g after the 7th cycle which results improved in comparison with those reported for $H_2Ti_3O_7$ electrodes, thus pointing to a protective effect of the amine.

1. Introduction

Titanium dioxide is one of the best-known transition metal oxide materials. TiO_2 has been extensively studied because of its excellent properties, among others, chemical stability, low cost, and no toxicity [1], as well as of its numerous applications, for instance, in photocatalysis [2] and energy conversion and storage [3].

Most prominent uses of this wide-gap semiconductor are strongly related to the energy of its valence and conduction bands. The photoexcitation of electrons from low laying valence band generate strong oxidant sites able to oxidize water and many organic compounds able to participate in photocatalytic processes useful, for instance, in water and air pollution remediation [4]. Rather low laying TiO_2 conduction band is in turn a good electron acceptor. This band may be easily populated, by chemical or electrochemical processes, thus generating electron donor centers able to participate in diverse chemical redox reactions and charge transfer phenomena, for example, in those involved in energy conversion by dye-sensitized TiO_2 based solar cells [5,6] or in the use of this oxide as electrode in lithium–ion batteries [7,8].

Important variables in the development of new, improved materials for most TiO_2 applications are both the size and shape of the particles. In the case of optical and catalysis processes, which are intrinsically surface phenomena, large surface to volume ratios are essential for obtaining high quantum yields and conversion efficiencies [9–11]. In electrochemical processes, where high electron and mass transport rates are needed, small particles with high surface areas appear to be also important, especially in the case of isolator oxides like TiO_2 where both electrical conductivity and lithium diffusion coefficients are rather low. Indeed, one-dimensional (1D) TiO_2 based nanomaterials have revealed to be interesting as active materials for potential applications [9,12,13]. So much work on the preparation of nanotubes and nanowires, generally obtained by strong alkaline treatment of precursors like anatase or rutile under hydrothermal conditions, has been reported [14–16]. However, studies on an eventual role of surfactants as

* Corresponding author at: Department of Chemistry, Faculty of Sciences, Universidad de Chile, P.O. Box 653, Santiago, Santiago, Chile. Tel.: +562 978 7404; fax: +562 271 3888.
E-mail address: ggonzale@uchile.cl (G. González).

0013-4686/$ – see front matter © 2009 Elsevier Ltd. All rights reserved.
doi:10.1016/j.electacta.2009.05.010

structure director, successfully used for instance in oxides like V_2O_5 [17], are in the case of the titanium dioxide still scarce [18]. Recently much attention has been paid to electrodes composed of titanate nanostructures which because of their layered structures are excellent hosts for lithium–ion intercalation, providing short path length for electron and lithium–ion transport, as well as of their good response to the strain of insertion–extraction process [19]. Large initial discharge capacities of $H_2Ti_3O_7$ based titanates, nanotubes and nanowires, which are near to the theoretical value of 1 mol lithium per mol TiO_2, has been reported [19–23].

In this work we describe some optical and electrochemical properties of $H_2Ti_3O_7$ organic–inorganic nanostructured composites prepared via the reaction of anatase with NaOH in the presence of the long-chain neutral surfactants, dodecylamine (DDA) and octadecylamine (ODA), that with the aim of evaluating its potentiality as materials for eventual photocatalitic or lithium-based energy storage applications. $H_2Ti_3O_7$ tubular nanostructures prepared by the methods described here are hybrid products containing amine which present both optical behavior and lithium uptake capacity similar to those of anatase nanostructures.

2. Experimental

2.1. Syntheses

0.4 g Anatase (Aldrich) with an equimolar amount or amine (DDA and ODA Aldrich 98%) were treated with 5 mL of 10 M NaOH (Merck) aqueous solution. Resulting suspensions poured in a Teflon lined autoclave were hydrothermically treated during different times, typically 12, 30, 48 and 72 h, at temperatures in the range 120–150 °C. Resulting solid white products were separated from the suspension by centrifugation, stirred in 0.1 M HCl for 24 h, washed repeatedly with deionized water until pH 6, and finally dried under vacuum (10^{-3} Torr). The products were analyzed by X-ray diffraction analysis (Siemens D-5000, Cu-K radiation), FT-IR (Bruker Vector 22 Fourier transform infrared spectrometer in the range 4000–250 cm^{-1} using KBr), SEM (Phillips XL-30), TEM (JEOL 100-SX, and FEI Tecnai F20) and elemental analysis (SISONS ES-1108). Elemental analysis for selected samples: DDA 130 °C, 48 h: % Found (calculated for $(H_2Ti_3O_7)(DDA)_{0.4}$): C: 16.74 (16.75); H: 4.63 (4.63); N: 1.88 (1.63). ODA, 130 °C, 72 h: % found (calculated for $(H_2Ti_3O_7)$ $(ODA)_{0.55}{\cdot}H_2O$): C: 23.73 (23.73); H: 6.56 (6.56), N: 1.55 (1.54). ODA, 150 °C, 72 h: % found (calculated for $(H_2Ti_3O_7)$): C: 0.31 (0.00); H: 1.22 (1.20), N: 0.16 (0.00).

2.2. Optical measurements

The diffuse reflectance UV–vis spectra were recorded using a Shimadzu UV–vis spectrophotometer, 2450 PC model, equipped with an integrator sphere. Barium sulfate was used in all cases as reference material, and spectra were recorded in the range of 200–800 nm with an aperture of 0.1 nm and media scanning speed at room temperature. Reflectance measurements were converted to absorption spectra using the Kubelka–Munk function. The photoluminescence (PL) spectra were recorded at room temperature using a PerkinElmer spectrofluorometer, MPF-2A model. This spectrometer is equipped with a 150 W xenon lamp source, emission and excitation monochromator, and photomultiplicator tube (R-106).

2.3. Electrochemical measurements

Working electrodes were prepared by pressing about 2–3 mg of a mixture of the sample with 15 wt% of pure carbon powder as conductive assistant material on a 0.3 cm^2 gold mesh. A piece of 7.5 mm thin lithium ribbon was used as both counter and reference electrode. Electrodes were separated by glass fiber soaked in 1 M $LiPF_6$ ethylene carbonate/dimethyl carbonate v/v electrolyte solution. The cells were assembled in a dry argon-filled globe box and kept hermetically sealed during the experiments. Intermittent galvanostatic discharge studies were performed at room temperature using a current density of 150 $\mu A\,cm^{-2}$ (Autolab Potentiostat-Galvanostat 12). The amount of intercalated lithium was determined coulommetrically. Quasi-equilibrium potentials were measured stepwise (1 h intercalation followed by 10 h rest under open circuit conditions) and referred to the Li/Li^+ electrode. Lithium chemical diffusion coefficients in samples were determined in the same cell by the galvanostatic pulse relaxation technique [24] at different temperatures in the range 15–40 °C. In these experiments, a constant current (i) is applied for a short time (τ), thus producing a concentration excess (λ mol/cm^2) of lithium on the surface of the titanat electrode. After interrupting the current, the time-dependent relaxation of the voltage (E) is measured. In order to meet the boundary conditions relevant to the solution of the diffusion equation, especially the semi-infinite boundary condition, the duration of pulse has to be short compared to $l^2/2D$ where l is thicknesses of the electrode and D the diffusion coefficient. Considering working experimental conditions – current pulse durations (τ) of 5–10 s and planar disk electrodes with thicknesses (l) in the range 0.02 mm – and assuming a low diffusion coefficient, D, for the intercalated lithium, the following relation was used for the determination of the lithium chemical diffusion coefficient in the samples:

$$nF(E - E_0) = RT\,\ln\left\{\frac{[C_0 + \lambda(\pi Dt)^{1/2}]}{C_0}\right\}\ \text{with}\ \lambda = \frac{i\tau}{nFA},$$

where n is the number of electrons per lithium mol reduced, F the Faraday constant, E_0 the voltage of the unperturbed electrode, C_0 the concentration of lithium in the solid, and A the surface area of the electrode.

Charge/discharge cycles at room temperature were performed at 70 mA/g (Arbin Instrument College Station, USA) with cut-off voltages of 1.0 and 3.0 V (versus Li/Li^+).

3. Results and discussion

3.1. TiO_2-based hybrid nanotubes

The hydrothermal treatment of anatase under alkaline conditions, NaOH 10 M, in the presence of long-chain alkylamines leads to a series of products with composition and morphology which depend on both temperature and duration of the treatment as well as on the nature of the amine. In general, at short reaction time (<12 h) and low relatively temperatures (<130 °C), mixtures containing pristine anatase and other not always identifiable nanostructured products are obtained. Reactions performed in absence of amine or using short-chain amines lead to products mainly containing particles, fibers, or rods. However the use of longer amines leads to the formation of tubular species in good yields.

Best results, considering the purity of the phases and the morphological homogeneity of the structures, are obtained using amines with alkyl chains larger than 12 carbon atoms, at temperatures of about 130 °C, and reaction times equal or longer than 40 h. Under these conditions it is possible to obtain pure phases containing tubular organic–inorganic nanocomposites. Therefore we focused our attention on the products formed in the presence of dodecyl (DDA) and octadecyl amine (ODA). At temperatures higher than 130 °C, the morphology and the composition of the products using these two amines are however different. As may be observed in Fig. 1, the formation of nanostructures in the presence of DDA is extremely sensible to both, the temperature and

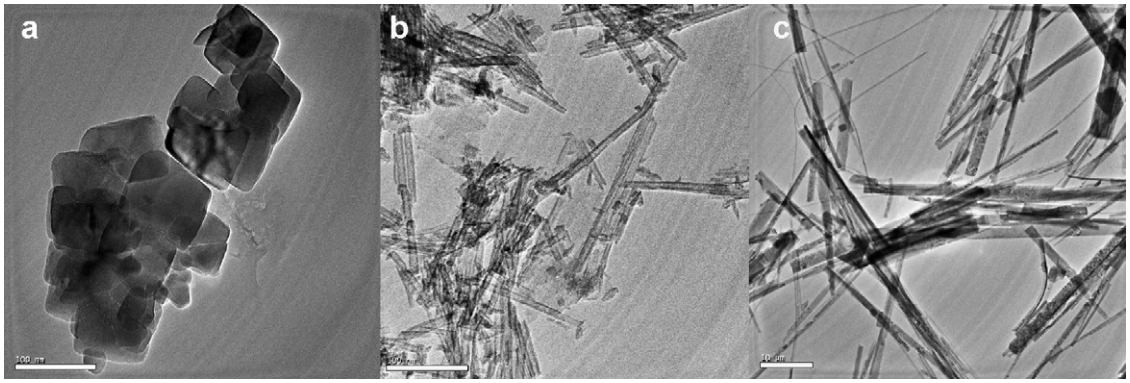

Fig. 1. TEM images of products obtaining in presence of DDA at 130 °C at different reaction times: (a) 30 h, (b) 48, and (c) 72 h.

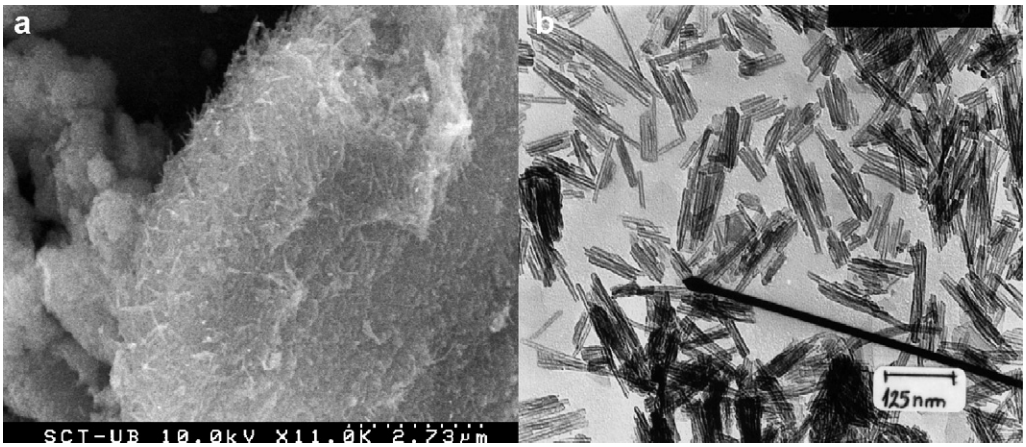

Fig. 2. Nanotubes prepared in the presence of DDA at 130 °C and a reaction time of 48 h: (a) SEM image of as prepared nanotubes and (b) TEM image of the same product after 10 min sonocation in ethanol.

the heating time under hydrothermal conditions. In general, pure phases were obtained only at reaction times longer than 40 h. Thus the product obtained at 130 °C after 30 h (Fig. 1a) contains a mixture of tubes, particles and pseudospherical arrangements. At reaction times in the range 40–50 h unique phases entirely constituted by tubular species as those illustrated in Fig. 1b are obtained. Yields are practically quantitative. Something similar occurs in the reaction performed in presence of ODA. In this case, a morphological pure phase constituted by spheres with diameters in the range 150–350 nm is apparent. However, X-ray diffraction analysis of the samples indicates the product corresponds to a mixture of species, principally $H_2Ti_3O_7$ nanotubes and its precursor anatase. So in this case, similarly to the reaction in presence of DDA mentioned above, the transformation of anatase into nanotubes appears to be completed only after 40 h reaction. There are however differences between the products prepared with DDA and ODA.

Nanotubes prepared with DDA are rather homogenous showing external and internal diameters of 10 ± 0.5 and 7.2 ± 0.5 nm respectively. Comparing Fig. 2a and b, which correspond to the same product before and after sonicating the sample during 10 min in ethanol respectively, it may be realized that the tubes are rather fragile. Moreover, the conditions under which these nanotubes may be isolated as a pure phase appear to be rather singular. Indeed longer reaction times make the tubes begin to collapse. So at 72 h a mixture containing majority fibers is obtained (Fig. 1c).

Nanotubes prepared with ODA (Fig. 3) are mechanically and thermally more stable than those obtained in the presence of DDA. Indeed they may be obtained in a wider range of reaction times, and their tubular morphology is preserved up to reaction times of 72 h. Indeed TiO_2-based tubular species are also produced at 150 °C when prepared in the presence of ODA.

As observed in Fig. 4, the XRD patterns of the nanotubes prepared with either DDA or ODA at 130 °C are similar. In spite of the rather low crystallinity of the samples, reflections which may be assigned to the species $H_2Ti_3O_7$ [22] are detected. Elemental analy-

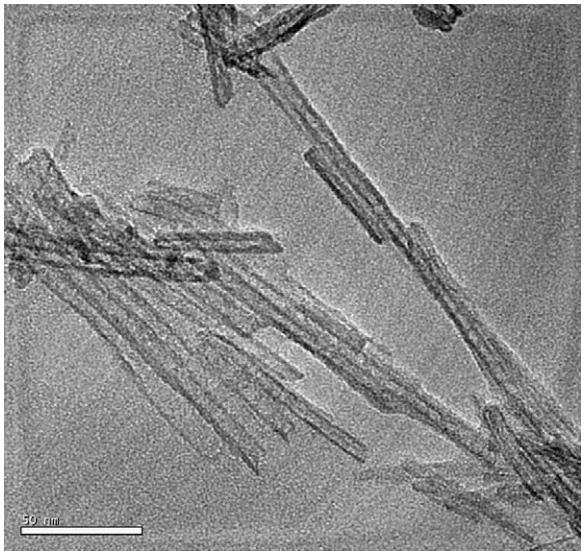

Fig. 3. TEM image of nanotubes obtained in the presence of ODA at 130 °C during 72 h.

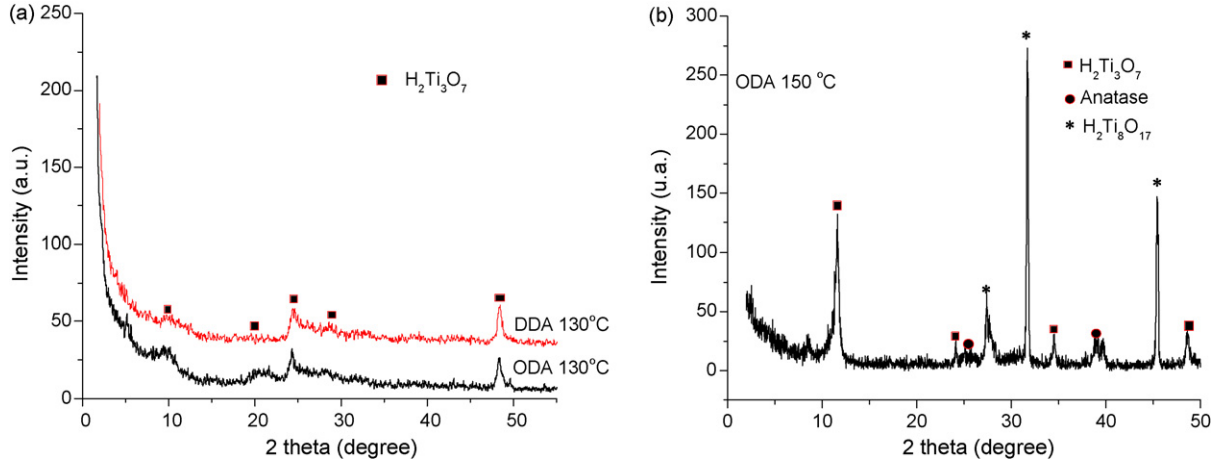

Fig. 4. X-ray diffraction patterns of nanotubes obtained in the presence of: (a) DDA and ODA at 130 °C and (b) ODA at 150 °C. Peak labeling from data-base JCPDS: $H_2Ti_3O_7$, 41-0192 [34]; H2Ti8O17 36-0656 [35]; Anatase, 83-2243 [36].

ses show that the products are TiO_2-amine nanocomposites which may be described by the general formula $H_2Ti_3O_7(amine)_x$ with x between 0.12 and 0.5. A typical FT-IR spectrum of these products is that displayed in Fig. 5, spectrum (a) corresponding to the DDA derivate. The absorption bands ν(N–H), ν(C–H) and δ(N–H) assignable to the amine may be clearly detected in the spectra agreeing with such a formulation. The fact that the presence of amine does not alter essentially the X-ray diffraction pattern of the $H_2Ti_3O_7$ nanotubes permits to conclude the organic component has to be inserted inside the tube but not in the interwall spaces.

As mentioned above, when the preparations are performed under more drastic conditions, about 70 h at 150 °C, the use of DDA leads only to fibers and wires. Meanwhile in the reaction performed with ODA, a practically quantitative formation of nanotubes is achieved. The X-ray diffraction pattern of this product is displayed in Fig. 4b. Although this product appears to be much more crystalline than that obtained at 130 °C, their XRD patterns are qualitatively similar. In both cases, reflections corresponding to the H-titanat $H_2Ti_3O_7$ are observed. However, in the product prepared in presence of ODA at 150, dehydration products as $H_2Ti_8O_{17}$ and anatase are also detected (Fig. 4b). Another important difference between the products obtained with ODA at 130 and 150 °C is the composition. Both FT-IR spectrum and elemental analysis indicate that the nanotubes obtained at 150 °C, contrarily to those prepared at 130 °C, do not contain amine. In order to test the role of the ODA in the formation of tubular species, the same experiment, 70 h, 150 °C, but without amine was performed. As observed in Fig. 6, only the formation of fibers was observed.

Results described above show that the first step in the formation of tubular nanostructures under strong alkaline conditions always consists in the formation of alkali titanates as being abundantly established in the literature [25–27], independently of the presence of the amine described here. The role of the amine appears to be essentially related to the stabilization of new phases like the spheres and the tubes containing amine as well as of the conventional nanotubes which, under the same conditions but without amine, leads principally to fibers.

3.2. Optical properties

Besides the exploration of the synthetic strategies leading to new nanostructured products in the form of nanotubes functionalized with the insertion of amines described above, it is interesting

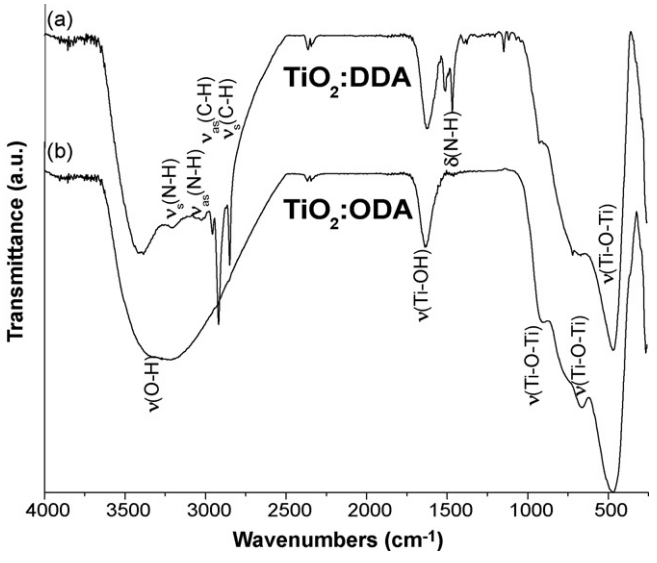

Fig. 5. FT-IR spectra of nanotubes obtained: (a) in the presence of DDA at 130 °C during 48 h and (b) in the presence of ODA at150 °C during 72 h.

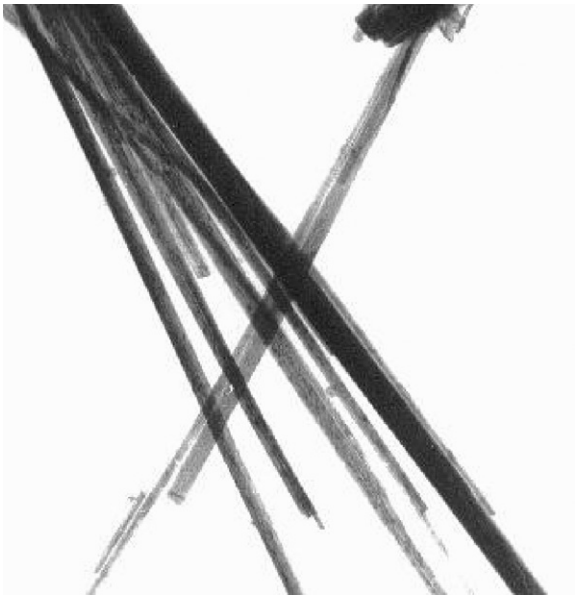

Fig. 6. TEM image of the product obtained at 150 °C during 72 h in absence of amine.

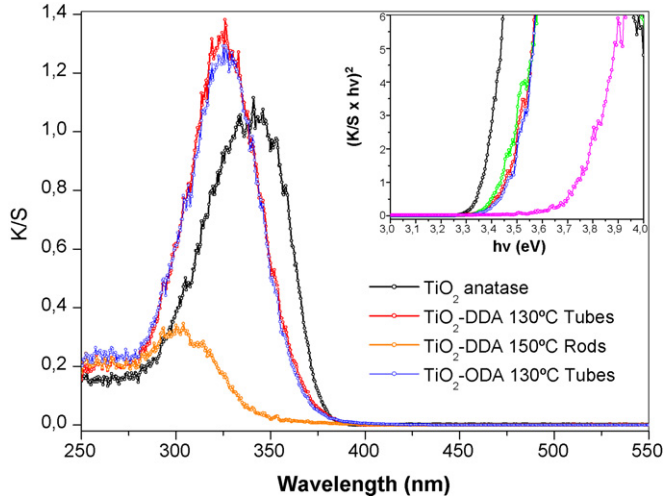

Fig. 7. Diffuse reflectance spectra of TiO_2 anatase and nanotubes after a Kubelka–Munk transformation (room temperature). The inset shows the $(K/Sh)^2$ vs. h, the intercept in h gives E_g values.

to analyze the optical properties of these nanocomposites; that in order to know if the presence of the amine alters significantly the electronic structure of the products. In the case of inorganic semiconductor derivatives, such studies are normally centered on the size-dependent optical properties, especially in the determination of the optical gap, as well as the photoluminescent properties of the products.

In Fig. 7 are reproduced the diffuse reflectance spectra, after Kubelka–Munk transformation [28], of a series of the products obtained during this study are compared with that of the pristine anatase. Although the shape of the spectra is in general the same, notorious differences in the absorption edges are observed. As expected, all these products behave as "quantum" materials in which the most prominent property is the displacement of the absorptions towards higher frequencies with decreasing size of the particle. Such an effect may be interpreted as a result of the variation of the band gap with the reduction of the particle size. It is well known that in particles with sizes in the order of the nanometer, a situation that can be seen as a frontier in the transit from the band description in conventional solids to the discrete energy levels proper of molecular species occurs; it is expected the optical gap should increases with decreasing particle size. An evaluation of the optical gap in the different products may be made from the plot $(K/Sh)^2$ versus energy displayed in the inset of Fig. 7. The absorption edge energy or optical band gap (E_g) corresponds to the intersection point between the baseline along the energy axis and the extrapolated line from the linear portion of the threshold. In all the cases the product absorption edges of the nanostructured species present characteristic blue shifts respect to that in the micrometric anatase. Interestingly, the band gap values observed for all tubular structures result to be similar, independently of their amine content, thus agreeing with the nature of the inorganic component which is the same in all these products.

In Fig. 8a may be observed the photoluminescence (PL) spectra of the products analyzed in this work. All spectra were performed under similar conditions, using an excitation wave length of 300 nm (4.13 eV). The samples exhibit a strong, wide PL signal in the range 350–550 nm. As shown for anatase as a typical example in Fig. 8b, the fitting of experimental PL spectra using seven Gaussian curves indicates the presence of different emission states. In the spectrum of anatase, the small band observed at about 393 nm (3.15 eV) is attributed to the emission band edge of free excitation (excitonic emission). This band is blue shifted in the nanotubes, agreeing with observed UV–vis spectra commented above. Two peaks of higher intensity centered at 423 and 486 nm are attributed to emissions arising from traps located in the band gap, which in turn mainly result from surface defects type oxygen vacancies [29,30]. It is interesting to observe that in all the cases the spectra of obtained nanostructured products are similar to that of the pristine anatase. In each of them practically the same features, number, location and structure of the bands, are observed; they only differ in the intensity of the bands. Like in anatase, the emission corresponding to the direct transition is practically not observed, only a low intensity shoulder at high energy could be considered to arise from direct recombination. Such behavior indicates that the nature of the traps is the same in all the products, i.e. defects in the inorganic component of the nanostructures present in the pristine oxide which do not varied with the treatment used for the preparation of the products. That is certainly possible considering the relatively soft method used in the preparations.

3.3. *Electrochemical insertion of lithium in H-titanat nanocomposites*

The variation of the quasi-equilibrium potential of the couple Li/Li^+ with the amount of intercalated lithium for studied nanocomposites, $(H_2Ti_3O_7)(DDA)_{0.4}$ and $(H_2Ti_3O_7)(ODA)_{0.55}\cdot H_2O$, is reported in Fig. 9. As observed, a change in the potential of about

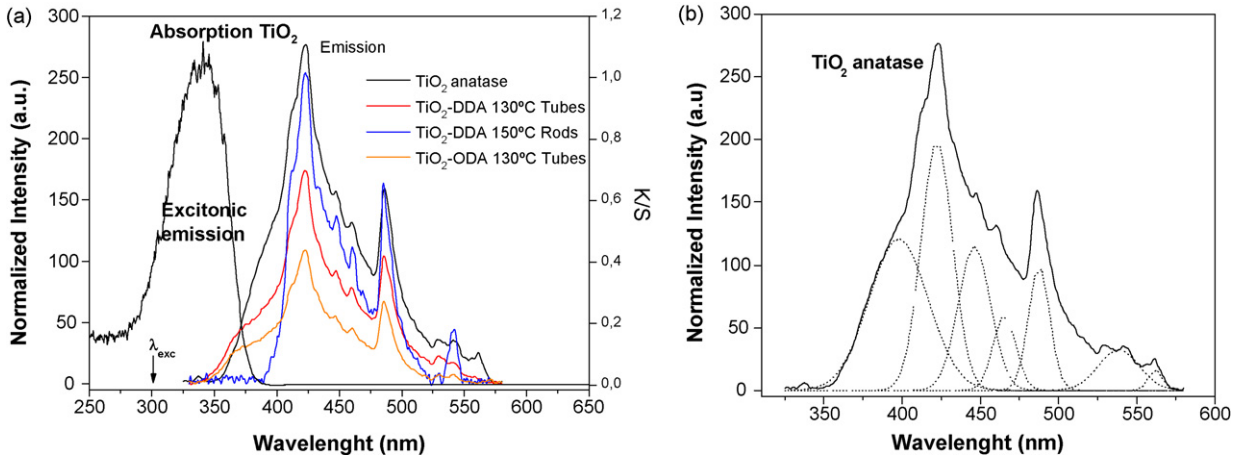

Fig. 8. (a) Photoluminescence spectra of the TiO_2 anatase and nanotubes with excitation at 300 nm. (b) Deconvolution in six Gaussian curves of the photoluminescence spectra of TiO_2 anatase.

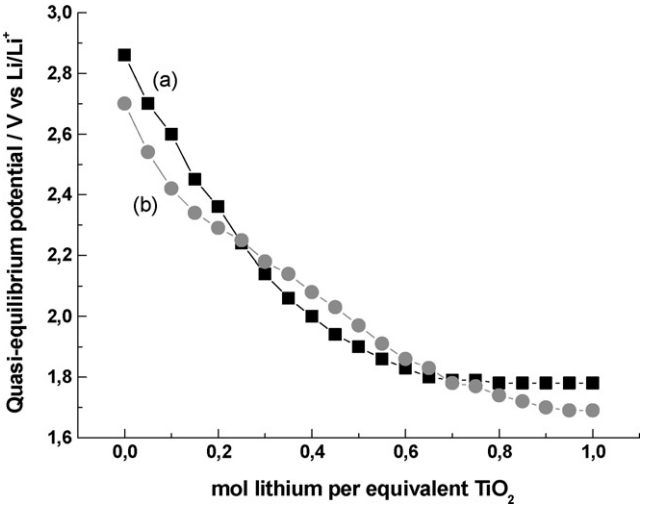

Fig. 9. Insertion of lithium into tubular hydrogen titanat nanocomposites. Quasi-equilibrium discharge voltages for nanotubes containing: (a) dodecylamine DDA and (b) octadecylamine ODA.

1.0 V is produced after the intercalation of 1 mol lithium per mol equivalent TiO_2. The variation of the voltage with the amount of inserted lithium is rather similar for both, DDA and ODA derivatives. That agrees with the fact that the inorganic environment of lithium ion in both systems is the same, because, as discussed above, the organic component in the composites is located in the central cavity of the nanotubes. However, some slight differences are observed in the range between 0.2 and 0.35 mol lithium per equivalent TiO_2. Indeed in the curve corresponding to the tubes containing ODA (curve b in Fig. 9) there are some slope changes which could be interpreted as consecutive phase changes probably produced by reorganization of the amine and/or the presence of water in the product.

The diffusion of lithium in both DDA and ODA $H_2Ti_3O_7$ $(amine)_x$ hybrid nanotubes also shows differences. In Fig. 10 is shown the variation of the chemical diffusion coefficients with the temperature for these two nanocomposites, both intercalated with the same amount of lithium, 0.1 mol lithium per equivalent TiO_2. The comparison of the values, 2.98×10^{-13} and 6.8×10^{-12} $cm^2\ s^{-1}$ corresponding to the products with DDA and ODA respectively, with those reported by Liu et al. for Li^+ ion insertion in nano-sized

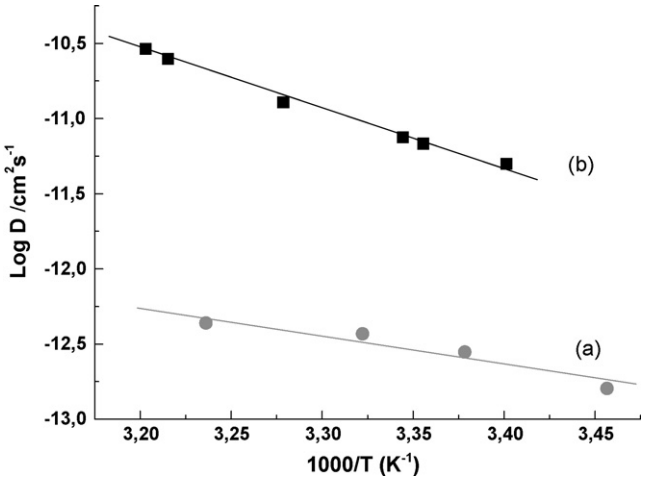

Fig. 10. Chemical lithium diffusion coefficients of lithium in organic–inorganic H-titanate nanotubes containing: (a) dodecylamine (DDA) and (b) octadecylamine (ODA).

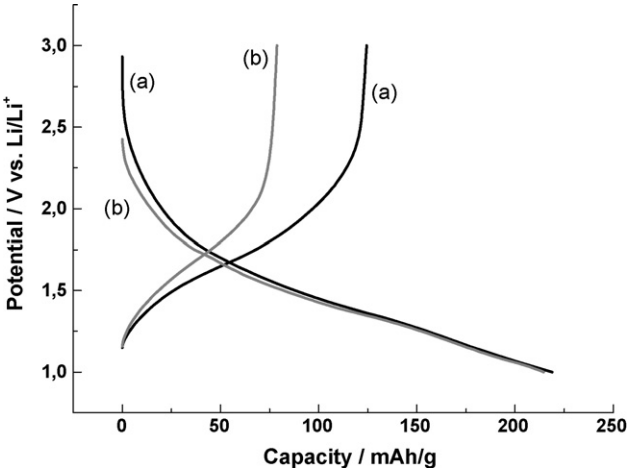

Fig. 11. First discharge–charge curves of hybrid organic–inorganic H-titanate nanotubes containing: (a) dodecylamine (DDA) and (b) octadecylamine (ODA).

TiO_2 (anatase) electrodes, 2.9×10^{-17} [31] shows that the former are encouraging higher. Interestingly, lithium diffusion appears to be somewhat favored in the compound with the longer amine. The diffusion occurs in the nanotube walls; however, because the large surface area/"bulk" ratio in this kind of structures, it can be expected that the diffusivity of lithium is also affected by interactions involving the inner surface of the tubes. Thus, a relatively more disordered arrangement of the organic component inside the tubes, due to a longer hydrocarbon chain, and the presence of water, apparently induced by the insertion of a longer amine, could be the reasons of the different diffusion coefficients observed in these two products.

The first discharge–charge curves for samples of the tubular nanocomposites $(H_2Ti_3O_7)(DDA)_{0.4}$ and $(H_2Ti_3O_7)(ODA)_{0.55}\cdot H_2O$ described here are displayed in Fig. 11. $H_2Ti_3O_7$ nanotubes are multilayered structures in which inter-wall spaces as well as outer and inner surfaces are covered with hydroxyl groups [32]; therefore, an irreversible reaction of these groups with lithium leading to a pronounced initial capacity loss is expected. As reported by Zhang et al. [20], as prepared $H_2T_{i3}O_7$ nanotubes present a first-cycle irreversible capacity of 142 mAh/g. This capacity loss, which is higher than that of titania nanoparticles [31,33], is reduced to 113 and 88 mAh/g when the samples are annealed to 200 and 300 °C respectively pointing clearly to the benefit effect of the loss of water on the capacity of these materials. The irreversible capacity of the DDA and ODA derivatives observable in Fig. 11 accounts 94 and 136 mAh/g respectively. Interestingly, the capacity loss in the first cycle for the DDA composite (curve a in Fig. 11) results to be lower than that already mentioned for the purely inorganic as prepared $H_2T_{i3}O_7$ nanotubes [20], thus pointing to a protective role of the amine against the reaction of lithium with the hydroxyl moiety in the product. However, the ODA nanocomposite displays an irreversible capacity which is comparable to that of as prepared $H_2Ti_3O_7$ nanotubes reported by Zhang et al. [20]. The fact that analytical determinations indicate that the nanotubes containing ODA, contrarily to those with DDA, retain water in its structure, agrees with the effect of water in the irreversible capacity of the material in dynamic discharge/charge processes.

In Fig. 12a and b is shown the variation of the capacity in the first and following 6 cycles for the products containing DDA and ODA respectively. The compound with ODA loses about 64% of its capacity in the first cycle. After the 7th cycle it reaches a value of 59.4 mAh/g (72% loss respect to the initial capacity). Meanwhile the loss of capacity of the DDA compound results to be comparatively much lower, 33% (72.4 mAh/g) in the first cycle and 48% (113 mAh/g)

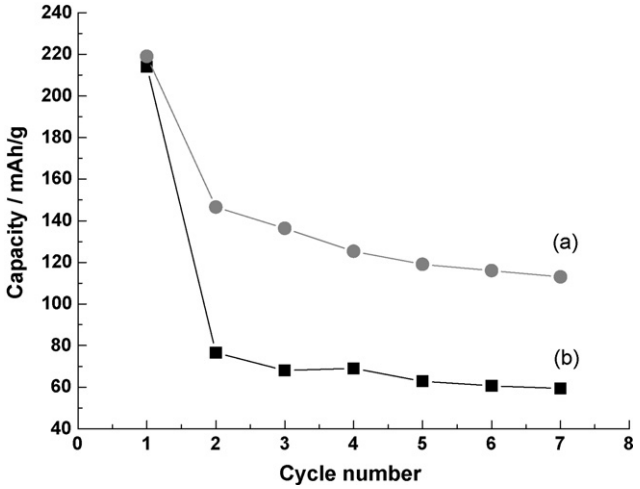

Fig. 12. Discharge/charge profiles of hybrid H-titanate electrodes: (a) dodecylamine (DDA) and (b) octadecylamine (ODA).

after the 7th one. During following cycles the capacity of the products slowly decreases, showing, after the 20th cycle, values of 110 and 55 mAh/g for the nanocomposites containing DDA and ODA respectively.

From results discussed above it is apparent that the length of the amine carbon chain plays a role in the electrochemical behavior of the tubular $H_2Ti_3O_7$-amine nanocomposites described here. The effects possibly occur directly altering the order in the structures and/or influencing the activity of the inner surface of the tubes as well as indirectly determining the amount of water retained by the structures. In order to get a better comprehension these issues and thus enhancing the possibility of formulating and attaining organic–inorganic nanocomposites with improved electrochemical properties, further experiments using other organic components, reactions conditions, and post-synthesis treatments are in progress.

4. Conclusions

The addition of appropriate long-chain amines to the reaction generally used for preparing nanostructures based on the hydrogen-titanate $H_2Ti_3O_7$ leads to nanotubes which contain amine incorporated in their structures. The products are a new kind of functionalized nanostructured TiO_2-based species. The type of structures, the purity of the phases, and the content of the organic component may be regulated by selecting both the reaction conditions and the length of the amine. The hybrid nature of these structures opens a new window in the applications of this wide gap semiconductor frequently used in fields like photocatalysis and energy storage and conversion.

The functionalization of TiO_2 with the amine appears to be a soft process in which the essential characteristics of this oxide are conserved. So the electronic spectra of these nanocomposites result to be similar to those of the nano- or microparticles, but showing absorption band edges shifted to higher energies, according to the characteristic size of the nanotubes, independently of the nature of the amine. The similitude of the optical behavior of TiO_2 micro and nanostructures is also appreciated in the photoluminescence spectra of the materials. All features characteristic of anatase may be observed at the same wave length in all these nanostructured products. The spectra are dominated by emissions arising from the presence of traps possibly located in the common inorganic component in all these structures.

The TiO_2 based hybrid tubular nanostructures are also able to host lithium up to about one lithium mol per equivalent TiO_2. However, the potential response to the intercalation of lithium of the nanocomposites results to be not the same for both derivatives. With the longer one, ODA, compositional and structural changes or disorders affecting both, the equilibrium voltage and the reversibility of the charge/discharge process are apparent, so the loss of capacity in the first cycle results about twice of that observed for the dodecylamine nanocomposite. Moreover, the irreversible capacity of the DDA nanocomposite results to be lower than that reported for as prepared $H_2Ti_3O_7$ nanotubes [20], a fact that could reflect a stabilizing effect of the organic component.

The method described here successes in functionalizing TiO_2 under conditions which are soft enough for maintaining the electronic structure of the pristine oxide in spite of the hybrid nature of the products.

Acknowledgments

Fondecyt (Grants 1090282, 1070195 and 7070162), Basal Financing Program for Scientific and Technological Centers of Excellence, CONICYT (CEDENNA), Millennium Science Nucleus P06-022-F, VIC Universidad de Chile (CSIC 21/09-10), and Universidad Tecnológica Metropolitana, are gratefully acknowledged.

References

[1] K. Narasimha Rao, Opt. Eng. 41 (2002) 2357.
[2] A. Mills, S. Le Hunte, J. Photochem. Photobiol. A: Chem. 108 (1997) 1.
[3] A.R. Armstrong, G. Armstrong, J. Canales, P.G. Bruce, Angew. Chem. Int. Ed. 43 (2004) 2286.
[4] O. Carp, C.L. Huisman, A. Reller, Progr. Solid St. Chem. 32 (2004) 33.
[5] B. O'Regan, M. Grätzel, Nature 353 (1991) 737.
[6] S. Nishimura, N. Abrams, B.A. Lewis, L.I. Halaoui, T.E. Mallouk, K.D. Benkstein, J. van de Lagemaat, A.J. Frank, J. Am. Chem. Soc. 125 (2003) 6306.
[7] G. Sudant, E. Baudrin, D. Larcher, J.M. Tarascon, J. Mater. Chem. 15 (2005) 1263.
[8] S.W. Oh, S.H. Park, Y.K. Sun, J. Power Sources 161 (2006) 1314.
[9] X. Chen, S.S. Mao, Chem. Rev. 107 (2007) 2891.
[10] J. Joo, S.G. Kwon, T. Yu, M. Cho, J. Lee, J. Yoon, T. Hyeon, J. Phys. Chem. B 109 (2005) 15297.
[11] J.M. Wu, Environ. Sci. Technol. 41 (2007) 1723.
[12] I.C. Flores, J.N. Freitas, C. Longo, M.A. De Paoli, H. Winnischofer, A.F. Nogueira, J. Photochem. Photobiol. A: Chem. 189 (2007) 153.
[13] Y.S. Hu, L. Kienle, Y.G. Guo, J. Maier, Adv. Mater. 18 (2006) 1421.
[14] Z.Y. Yuan, J.F. Colomer, B.L. Su, Chem. Phys. Lett. 363 (2002) 362.
[15] Y.X. Zhang, G.H. Li, Y.X. Jin, Y. Zhang, J. Zhang, L.D. Zhang, Chem. Phys. Lett. 365 (2002) 300.
[16] R. Yoshida, Y. Suzuki, S. Yoshikawa, J. Solid State Chem. 178 (2005) 2179.
[17] C.O. Dwyer, D. Navas, V. Lavayen, E. Benavente, M.A. Santa Ana, G. González, S.B. Newcomb, C.M. Sotomayor Torres, Chem. Mater. 18 (2006) 3016.
[18] H. Lozano, E. Benavente, G. González, J. Nanosci. Nanotech. 9 (2009) 969.
[19] M. Wei, K. Wei, M. Ichihara, H. Zhou, Electrochem. Commun. 10 (2008) 1164.
[20] H. Zhang, G.R. Li, L.P. An, T.Y. An, X.P. Gao, H.Y. Zhu, J. Phys. Chem. C 111 (2007) 6143.
[21] J.R. Li, Z.L. Tang, Z.T. Zhang, Chem. Mater. 17 (2005) 5848.
[22] B.L. Wang, Q. Chen, J. Hu, H. Li, Y.F. Hu, L.M. Peng, Chem. Phys. Lett. 406 (2005) 95.
[23] A. Armstrong, G. Armstrong, J. Canales, R. García, P. Bruce, Adv. Mater. 17 (2005) 862.
[24] S. Basu, W.L. Worrel, in: P. Vashista, J.N. Mundy, G.K. Shenoy (Eds.), Fast Ion Transport in Solid, Elsevier, Noth Holland, 1979, p. 149.
[25] G.H. Du, Q. Chen, R.C. Che, Z.Y. Yan, L.M. Peng, Appl. Phys. Lett. 79 (2001) 3702.
[26] T. Kasuga, M. Hiramatsu, A. Hoson, T. Sekino, K. Niihara, Langmuir 14 (1998) 3160.
[27] M. Wei, Y. Konish, H. Zhoua, H. Sugihara, H. Arakawa, Solid State Commun. 133 (2005) 493.
[28] W.W. Wendlant, H.G. Hecht, Reflectance Spectroscopy, Interscience, New York, 1966.
[29] J. Liqiang, Q. Yichun, W. Baiqi, L. Shudan, J. Baojiang, Y. Libin, F. Wei, F. Honggang, S. Jiazhong, Sol. Energy Mater. Sol. Cells 90 (2006) 1773.
[30] J. Xu, L. Li, Y. Yan, H. Wang, X. Wang, X. Fu, G. Li, J. Colloid Interface Sci. 318 (2008) 29.
[31] Z. Liu, L. Hong, B. Guo, J. Power Sources 143 (2005) 231.
[32] Q. Chen, W. Zhou, G. Du, L.M. Peng, Adv. Mater. 14 (2002) 1209.
[33] O. Wilhelm, S.E. Pratsinis, E. de Chambrier, M. Crouzet, I. Exnar, J. Power Sources 134 (2004) 197.
[34] V. Nalbandyan, et al., Russ. J. Inorg. Chem. Eng. Trans. 32 (1987) 639.
[35] H. Izawa, et al., J. Chem. Phys. 86 (1982) 5023.
[36] V.I. Khitrova, et al., Kristallografiya 22 (1977) 1253.